A two-frame approach for scene-based nonuniformity correction in array sensors

Chao Zuo [a,b], Yuzhen Zhang [a,*], Qian Chen [a,b], Guohua Gu [a], Weixian Qian [a], Xiubao Sui [a], Jianle Ren [a]

[a] Jiangsu Key Laboratory of Spectral Imaging & Intelligence Sense, Nanjing University of Science and Technology, Nanjing, Jiangsu Province 210094, China
[b] Key Laboratory of Photoelectronic Imaging Technology and System, Ministry of Education of China, Beijing Institute of Technology, Beijing 100081, China

HIGHLIGHTS

- We introduce a new scene-based technique to correct the fixed-pattern noise in array sensors.
- This method register a pair of image frames exhibiting small translation.
- The noise pattern can be reconstructed using constrained least squares estimation.
- Accurate estimates of the bias nonuniformity can be achieved with only two frames.

ARTICLE INFO

ABSTRACT

This paper introduces a new scene-based technique to correct the fixed-pattern noise (FPN) in array sensors. This method registers a pair of image frames exhibiting small relative scene translation and then the noise pattern can be reconstructed using the constrained least-squares estimation. The key advantage of this technique is that the accurate estimates of the bias nonuniformity can be obtained with only two images, without imposing any assumptions on the structure of the FPN. Besides, the method works on almost static scene, and therefore does not require larger scale global motion and statistical assumptions on the scene irradiance. We test our method on synthetically generated FPN as well as with real infrared data, and experimental results demonstrate the significant reduction in FPN, validating the effectiveness of our approach. Finally, we validate the feasibility and validity of using the proposed method as a first step fostering the success of more sophisticated registration-based time-evolving correction algorithms.

Crown Copyright © 2013 Published by Elsevier B.V. All rights reserved.

1. Introduction

Focal-plane array (FPA) sensors have become the most prominent detector used in infrared (IR) and visible-light imaging systems in recent years. However, FPA sensors, especially IRFPA are strongly affected by the nonuniform spatial response of each pixel sensor which arises due to the different responses of each photodetector within a FPA sensor [1,2]. This nonuniformity problem represents the main cause of fixed pattern noise (FPN) which is easily noticeable in the acquired images. Furthermore, for uncooled infrared cameras the problem is even worse because the nonuniformity of the sensor response is not stationary and often drifts with time. For this kind of camera, scene-based nonuniformity correction (SBNUC) is required throughout the sensor operation to eliminate the influence of temporal drift without interrupting its normal operation.

Numerous scene-based nonuniformity correction techniques have been developed over the years. Such algorithms are generally identified by two main approaches, namely, statistical methods [1–6] and registration-based methods [7–9]. Statistical methods usually impose some spatiotemporal assumptions on the irradiance collected by each detector in the array, and then some quantities are extracted to estimate the correction coefficients for the FPN. For example, the temporal high-pass filtering method [1] assumes that the FPN should reside in the low temporal frequency domain while the real scene not. The constant-statistics method [4] assumes that, over time, the mean and variance of the irradiance of the scene become spatially invariant. The constant-range method [6] is based on the assumption that all pixel locations are exposed to the same range of possible values within a sequence of frames. Scribner's algorithm [3] employed the ideal that the real scene should spatially local smooth and belongs to the high temporal frequency domain, but with the FPN the opposite is true. A common drawback of these methods is the requirement of a large number of frames and the camera needing to move in such a way in order to satisfy the spatiotemporal assumptions made. To ensure these

spatiotemporal assumptions stand, statistical algorithms typically require a large number of frame samples (hundreds of frames), particular conditions of observation, and sufficiently random camera motion [10].

The registration-based methods, however, consider that each detector should have identical response when observing the same scene position and the response difference between the two detectors is due to the FPN. Evidently, this assumption is much less stringent than the ones made by statistical methods, therefore registration-based methods are more efficient in terms of the number of frames used for parameter estimation. The first registration-based method technique developed by Hardie et al. [7] employs the idea that the average of properly registered observed image frames gives an unbiased estimate of the true scene based on simplified assumptions of identical Gaussian distributions of parameters from pixel to pixel. Ratliff et al. [8] proposed a algebraic SBNUC algorithm which uses pairs of image frames that exhibit arbitrary one-dimensional or two-dimensional translational motions to help remove non-uniformity in the bias of the FPA response. Recently, we presented an interframe-registration-based algorithm (IRLMS) [9] in which NUC could be achieved by estimating the global translation between two adjacent frames and minimizing the mean square error between the two properly registered images.

Since both approaches rely on some assumptions about the scene observed, they are susceptible to ghosting artifacts when the undying assumptions break down. This problem is more serious among statistical methods and several some solutions for reducing ghosting effect have been proposed: A simple deghosting method is to detect the changes between frames and deselect the input image if the change is less than a threshold [11], which has been proven to be effective but still insufficient. Some methods introduce spatial filtering into temporal high-pass filtering method [12–14] and constant statistic method [10,15] to reduce ghosting, considering local statistics assumptions are much easier to be satisfied than the global ones. The adaptive learning rate [16], edge-preserving spatial filter [17], and temporal statistics thersholding [18] strategies have been introduced in the Scribner's algorithm to preventing ghosting artifacts and object degeneration. On the other hand, the ghosting effect in registration-based methods appears less serious, but it also still nonnegligible. A recent work improved IRLMS method by introducing three strategies to reduce the ghosting effect resulting from inaccuracy of registration, local motion, scene warping and rotation, etc. [19].

The above mentioned NUC methods, both statistical methods and registration-based methods are known collectively as time-evolving SBNUC, wherein a relatively larger number of image frames (even for registration methods, at least tens of frames are required) are needed to estimate the NUC parameters reliably, in a recursive matter. Quite different from the time-evolving SBNUC, some single frame SBNUC method are proposed recently to correct FPN with only single capture and thus no camera/scene motion and no registration is required [20–22]. Besides, they are free from the ghosting problem because their single-frame property. However, these methods are only limited to the one-dimensional case (stripe nonuniformity) and of little avail when the FPN is arbitrary two-dimensional pattern.

The propose of this paper is to present a novel scene-based NUC method, two-frame NUC (TFNUC), wherein NUC can be achieved employing only two image frames which exhibit a small relative scene translation. Since our method employ image registration, it should be categorized into the registration-based SBNUC. But more strictly speaking, it constitutes a class by itself, falling in between the time-evolving SBNUC and single-frame SBNUC, because the complete, non-recursive NUC can be achieved with only two image frames, without imposing any assumptions on the structure of FPN. We introduce the principles of the new method; and simulations and experimental results are given to verify the effectiveness of the TFNUC method. Some practical considerations and potential applications of the proposed method will be also discussed.

2. Proposed method

Consider $s_1(x, y)$ as a two-dimensional (2-D) scene image defined in continuous space with real-number indices x and y. Because of the small camera motion or jitter, there is a small relative scene translation (strictly horizontal or vertical global motion) between a pair of consecutive frames observed during a rather short time. Let (δ_x, δ_y) represent this displacement in x and y directions respectively. If we choose the coordinate system of $s_1(x, y)$ as the reference coordinate system, then the displaced scene image in the camera's field of view can be represented as $s_2(x, y) = s_1(x - \delta_x, y - \delta_y)$. Thus the corresponding two observed frames can be defined as:

$$f_1(x, y) = s_1(x, y) + o(x, y) + n_1(x, y); \tag{1}$$

and

$$f_2(x, y) = s_2(x, y) + o(x, y) + n_2(x, y). \tag{2}$$

Since laboratory measurements have demonstrated that the offset component is the dominant source of FPN [7,8], we assumed a unitary gain. $o(x, y)$ stands for the offset nonuniformity which is signal independent and assumed to be fixed between two observed images. The term n_1 and n_2 correspond to the additive temporal noise, which are assumed to be signal independent. The FPN and additive temporal noise are also assumed mutually independent. It is noted that these conditions are valid in general applications. According to the shift property of Fourier transform:

$$S_1(u, v) = S_2(u, v)e^{-j(u\delta_x + v\delta_y)}, \tag{3}$$

where we adopt the notation of upper case letters for the corresponding Fourier-transformed function. Further, if the $f_2(x, y)$ is shifted in frequency domain properly, and then subtracted by the Fourier transform of $f_1(x, y)$, it follows that:

$$\begin{aligned} F(u, v) &= F_1(u, v) - F_2(u, v)e^{-j(u\delta_x + v\delta_y)} \\ &= O(u, v)\{1 - e^{-j(u\delta_x + v\delta_y)}\} + N(u, v). \end{aligned} \tag{4}$$

The term $N(u, v)$ is the combination of the two noise terms and equals to $N_1(u, v) - N_2(u, v)e^{-j(u\delta_x + v\delta_y)}$. Since $n_1(x, y)$ and $n_2(x, y)$ are signal independent, $n(x, y)$ should also be signal independent. Note that Eq. (4) fits the mathematical model of image degradation [23] very well and the block diagram is shown in Fig. 1. We rewrite Eq. (4) in spatial domain:

$$f(x, y) = o(x, y) * h(x, y) + n(x, y), \tag{5}$$

where $*$ represents the convolution operation. In image recovery problem, $h(x, y)$ is commonly referred as degradation operator and its Fourier transform, which is known as the degradation function, can be obviously expressed as below:

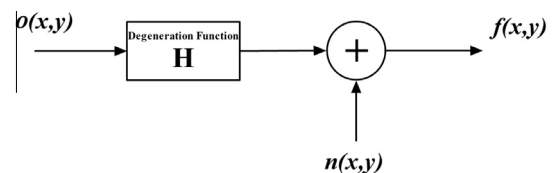$$H(u, v) = 1 - e^{-j(u\delta_x + v\delta_y)}. \tag{6}$$

Fig. 1. The block diagram for the image degradation model.

Note the above discussion is limited to the continuous case. When dealing with digital images, (x, y) are specified only in finite size discretized arrays $(N \times M)$. However, replacing the Fourier transform by the discrete Fourier transform (DFT), and also assuming a periodic extension of the images outside their compact support, it follows immediately upon substituting $u = \frac{2\pi k}{N}$ and $v = \frac{2\pi l}{M}$ that the degradation function becomes as below:

$$H(k,l) = 1 - \exp\left[-j\left(\frac{2\pi k}{N}\delta_x + \frac{2\pi l}{M}\delta_y\right)\right], \tag{7}$$

where $k = 0, ..., N - 1$ and $l = 0, ..., M - 1$. Similarly, Eq. (4) should be rewritten as:

$$F(k,l) = F_1(k,l) - F_2(k,l)\exp\left[-j\left(\frac{2\pi k}{N}\delta_x + \frac{2\pi l}{M}\delta_y\right)\right]$$
$$= O(k,l)\left\{1 - \exp\left[-j\left(\frac{2\pi k}{N}\delta_x + \frac{2\pi l}{M}\delta_y\right)\right]\right\} + N(k,l). \tag{8}$$

Then the continuous version of the degradation system for two-dimensional signals formulated in Eq. (5) can be expressed in discrete form by replacing the continuous arguments with arrays of samples in two dimensions. In this case, it is convenient for image recovery purposes to represent the discrete formulation of Eq. (5) as a system of linear equations, which expressed as [24]:

$$\boldsymbol{f} = \boldsymbol{Ho} + \boldsymbol{n}, \tag{9}$$

where $\boldsymbol{f}$, $\boldsymbol{o}$, and $\boldsymbol{n}$ are the lexicographic row-stacked versions of the discretized versions of $f(x, y)$, $o(x, y)$, and $n(x, y)$ and $\boldsymbol{H}$ is the degradation matrix composed of the $h(x, y)$.

In the presence of FPN, a fairly accurate estimates of (δ_x, δ_y) can be obtained with the image registration technique described in detail in [25]. At first glance, the solution to the signal recovery problem seems to be straightforward if $\boldsymbol{H}$ can be obtained precisely – find the inverse of the matrix $\boldsymbol{H}$ to solve for the unknown vector $\boldsymbol{o}$. However, it turns out that the solution is not so simple because in practice the degradation matrix is usually ill-conditioned or rank-deficient and the problem of inconsistencies or noise must be addressed. Fig. 2 shows the 3D plots of the magnitude of degradation function $H(k, l)$, with $(\delta_x, \delta_y) = (0.5, 0.5)$ and $(1.3, 2.7)$ (the zero-frequency component is shifted to center of spectrum). It can be seen that $H(k, l)$ assumes zero along some specific lines, which means that at these frequencies the information of $\boldsymbol{o}$ is unrecoverable. Particularly, the origin $(0, 0)$ is always on the zero lines, so we cannot get the direct current (DC) part of the FPN. However, it is not a problem because the offset FPN is usually assumed zero-mean without loss of generality. Another problem is, in practical applications, there are many uncertain factors, such as random noise, registration error, and tiny inconsistence of between the two scene images. Even small amount of errors may lead to a meaningless estimate with huge high frequency perturbations.

Regularization is one way to avoid the problems associated with inverting ill-conditioned degradation operators for signal recovery. The regularized solution of the inverse problem can be equivalently formulated by the following regularization-based least-squares problem [26]:

$$\hat{\boldsymbol{o}} = \arg\min_{O}\left\{\|\boldsymbol{o} - \boldsymbol{Hf}\|_2^2 + \gamma\|\boldsymbol{Qo}\|_2^2\right\}, \tag{10}$$

where the hat is used to denote an estimated value. The data fidelity item $\|\boldsymbol{o} - \boldsymbol{Hf}\|_2^2$ is the L_2 norm $(\boldsymbol{o} - \boldsymbol{Hf})^T(\boldsymbol{o} - \boldsymbol{Hf})$. $\|\boldsymbol{Qo}\|_2^2$ is the prior item. γ is commonly referred as the regularization parameter, which controls the tradeoff between fidelity to the data and the prior item. $\boldsymbol{Q}$ is known as the regularization matrix and one typical choice of $\boldsymbol{Q}$ is the Laplacian operator. By taking derivative with respect to $\boldsymbol{f}$, the solution for this overdetermined set of equations (Eq. (10)) becomes as:

$$\hat{\boldsymbol{o}} = [\boldsymbol{H}^T\boldsymbol{H} + \gamma\boldsymbol{Q}^T\boldsymbol{Q}]^{-1}\boldsymbol{H}^T\boldsymbol{f}. \tag{11}$$

The regularization parameter γ in Eq. (11) plays a very important role in the restoration process. Fig. 3 shows the examples of reconstructed offset image using Eq. (11) with three different regularization parameters. From Fig. 3, it can be seen that a small value of γ results in amplified errors in the estimated offset image. On the other hand, a large γ helps to suppress error while the nonuniformity would not be fully recovered. Since we can get the offset estimates with different γ, the corresponding corrected images can also be obtained. A proper γ should be chosen to provide best quality of the corrected image. The roughness index (ρ) is often used as a reference-free method to evaluation the quality of the corrected image [9,16]. So the optimal value of γ can be determined according to the follows criteria:

$$\hat{\gamma} = \arg\min_{\gamma}\rho(\gamma) = \arg\min_{\gamma}\left\{\frac{\|\boldsymbol{h}_1 * \hat{\boldsymbol{s}}_1(\gamma)\|_1 + \|\boldsymbol{h}_1^T * \hat{\boldsymbol{s}}_1(\gamma)\|_1}{\|\hat{\boldsymbol{s}}_1(\gamma)\|_1}\right\}, \tag{12}$$

where $\hat{\boldsymbol{s}}_1(\gamma)$ is estimated true scene two-dimensional image matrix without FPN, which can be obtained via $\boldsymbol{f}_1 - \hat{\boldsymbol{o}}(\gamma)$, $\boldsymbol{h}_1$ is a horizontal mask $[-1, 1]$, $\|\cdot\|_1$ is the L_1 norm, and $*$ represents discrete convolution. A typical curve of $\rho(\gamma)$ is illustrated in Fig. 4. It is not difficult to understand, if γ is too small, the high-frequency offset estimate error will result in an increase of the roughness index, whereas if γ is too large, the effect of non-uniformity correction will be weakened, $\rho(\gamma)$ will become larger too. The search of that minimum value can be achieved by a Newton–Raphson-like procedure [26] iteratively until $|\rho(\gamma_i) - \rho(\gamma_{i-1})| < a$, where a determines the final accuracy. Convergence to the optimal value of γ is usually achieved in 4–7 iterations, depending on the initial choices of γ and the accuracy parameter a.
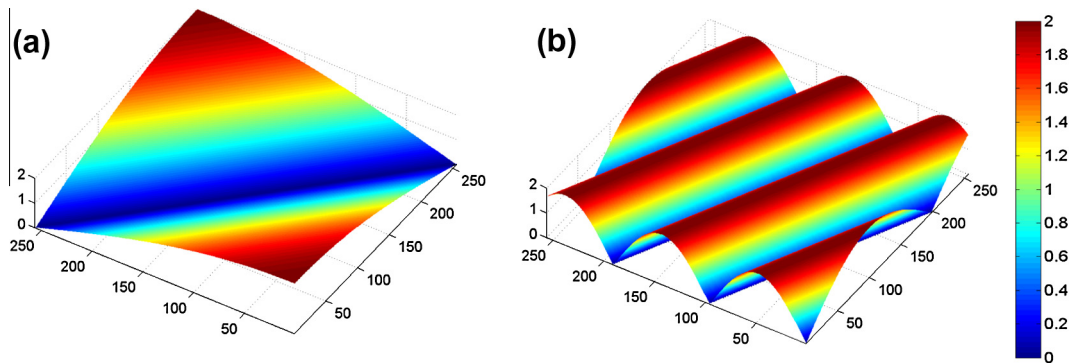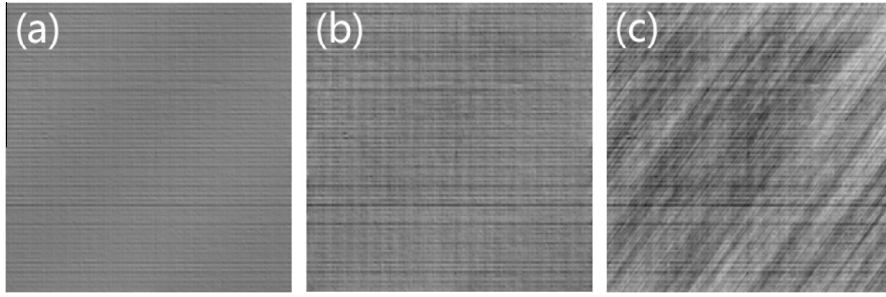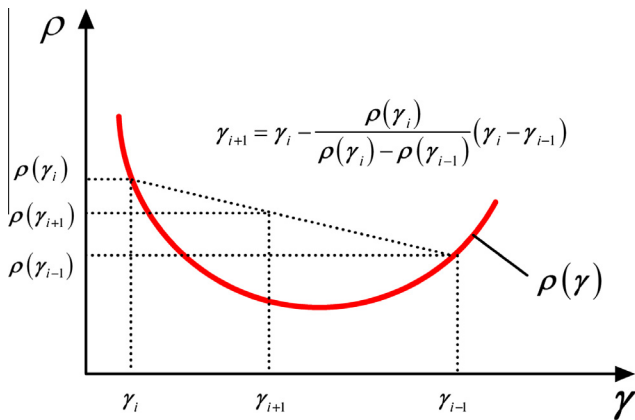

Fig. 2. The magnitude of the degradation function, when (a) $(\delta_x, \delta_y) = (0.5, 0.5)$ and (b) $(\delta_x, \delta_y) = (1.3, 2.7)$.

Fig. 3. Three reconstructed offset images with three different regularization parameters. (a) Regularization parameter that is too large. (b) Proper regularization parameter. (c) Regularization parameter that is too small.

Fig. 4. Iterative scheme for determination of γ. The two previous values are used to project the next value of γ.
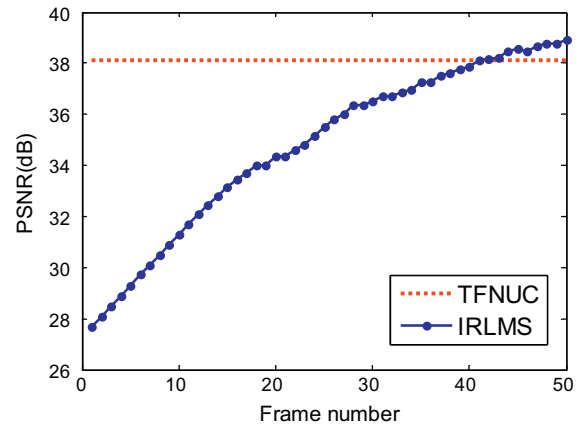
Fig. 5. PSNR results of the synthetic noisy test sequence.

3. Results

We present results over simulated and real IR image data. First, a 50-frame clean video sequence was captured using a well-calibrated mid-wave IRFPA camera. The sequence originally contained scene global motion introduced by moving the camera. This clean video sequence was artificially corrupted by Gaussian distributed offset nonuniformity. The PSNR value for the noisy raw images is 27.8 dB. We compared the performance of the proposed algorithm with IRLMS [9]. The metrics used to measure the NUC performance are given by the peak signal-to-noise ratio (PSNR) and the roughness index [9,16]. IRLMS was initialized with unitary gain, null offset, and a step size of 0.05. Its correction video can be found in Video 1, replayed at 5 frames per second. For the proposed method, the correction was performed using *only the last two frames*. Since best regularization parameter γ needs to be determined by Newton–Raphson searching, to clearly demonstrate the γ evolution and how the regularization parameter could affect the final correction result, the regularization parameter searching process with the corresponding corrected images are animated in Video 2. In this video, the raw last two frames from the 50-frame video sequence are displayed at the very beginning. Two values $\gamma_1 = 1$ and $\gamma_2 = 0.01$ were used as the initial values for projecting the next value of γ, and the accuracy parameter a was chosen as 0.001. The video shows the quality of the corrected image gradually improved with the regularization parameter approaching to the optimal value. The optimal value of γ was obtained as 0.032, after 7 iterations. Then the estimated offset was applied to all the 50 noisy images. Fig. 5 shows the PSNR curves of the two methods as a function of the frame number. It can be seen our method achieved a constant image quality of 38.1 dB, while the IRLMS method took about 43

frames to reach the same level. The final PSNR obtained by IRLMS is 38.9 dB, after 50 times iterations. For better illustration of the correction performance, the corrected images of the last frame (50th) of both methods are shown in Fig. 6. The results show that although the proposed TPNUC method used only two frames to estimate the nonuniformity coefficients, it gave a comparable NUC result with IRLMS wherein the correction was performed by analyzing 50 noisy frames.

We also tested the proposed method using real IR images with unknown FPN collected by two 320×256 HgCdTe FPA cameras operating in the 3–5 μm and 8–14 μm range, respectively. We captured two groups of noisy images, and each group includes two images exhibiting a small relative scene translation. Fig. 7a and c shows one of the two raw images of each group, from which stripe-like fixed pattern noise can be seen clearly. The striped patterns in the raw frame are mainly due to the readout architecture of the IRFPA – the photo-detectors along one column are grouped and multiplexed into each output channel by means of different readout amplifier circuits. Corrected images are presented in Figs. 7b and d, respectively. Two evolution videos are also presented (Videos 3 and 4), using the same parameter as our simulation. It can be seen TFNUC always shows a significant FPN reduction and the visual quality of the corrected images is satisfactory, as confirmed by the low roughness value displayed.

4. Other practical considerations

As one of many scene-based nonuniformity correction techniques developed, our method should find its ground of practical applications in this area. The most important characteristic of our method is that only two frames are needed to perform a complete correction, without imposing any assumption and pre-knowledge
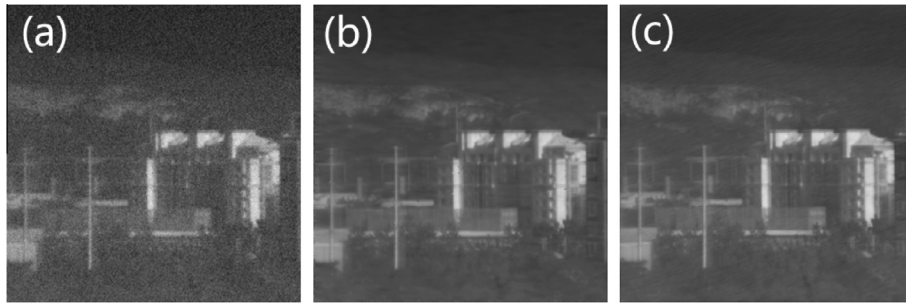
Fig. 6. NUC results on the simulated test images. (a) RAW frame 50: PSNR = 27.8 dB, ρ = 0.272. (b) IRLMS: PSNR = 38.9 dB, ρ = 0.092. (c) TFNUC: PSNR = 38.1 dB, ρ = 0.096.
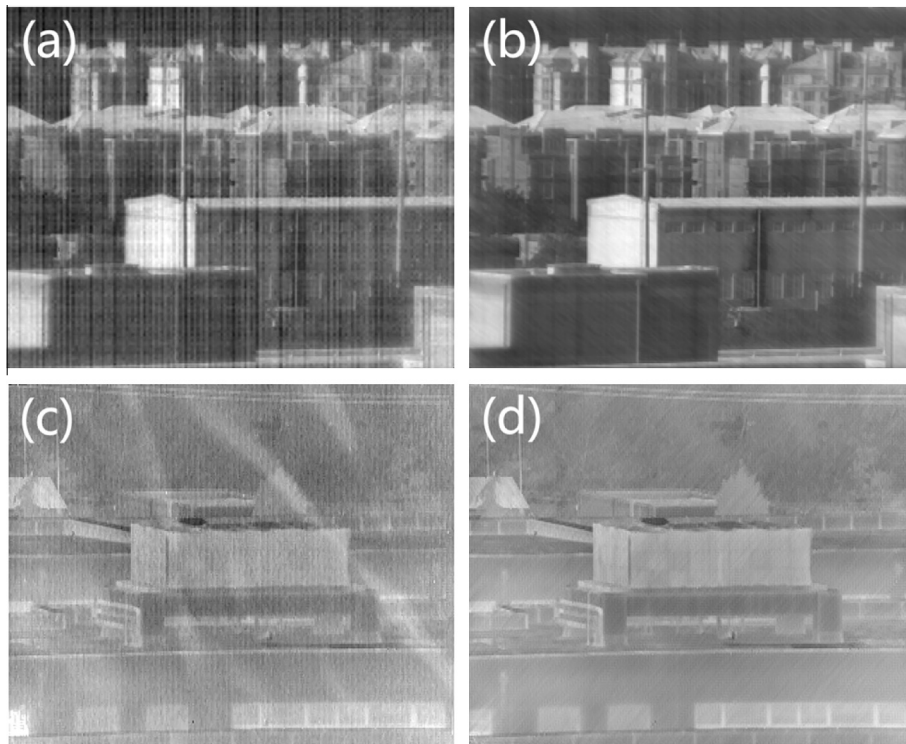

Fig. 7. NUC results on real IR images: (a) RAW frame: ρ = 0.231, (b) TFNUC: ρ = 0.139, (c) RAW frame: ρ = 0.157, and (d) TFNUC: ρ = 0.089.

about the characteristic of the nonuniformity. So it is well-suited for the applications of recovering the underlying true signals from the limited acquired data contaminated by FPN, as a post-processing algorithm. Despite its high efficiency in reducing the frame number needed, it is not a wise idea to perform our method recursively due to its relatively high computational complexity. Besides, since only two frames are employed to estimate the correction parameters, the NUC accuracy of our method is undoubtedly cannot go higher than some other time-evolving methods wherein the correction parameter can be estimated by analyzing tens, or even hundreds of image frames. Given all this, we believed our method is more suitable for to be a pre-correction SBNUC method, used along with other time-evolving methods. Once the camera starts, our method is performed as a first step to quickly reduce the initial FPN, and then other time-evolving methods can be then applied to further refine the correction parameters and follow the temporal drift of FPN. Such a combination could significantly increase the convergence rate of the time-evolving method, producing substantially clear and virtually usable images for observation purposes within only two-frame time interval. And meanwhile, the combination will not affect the steady-state accuracy and long-term performance of the NUC.
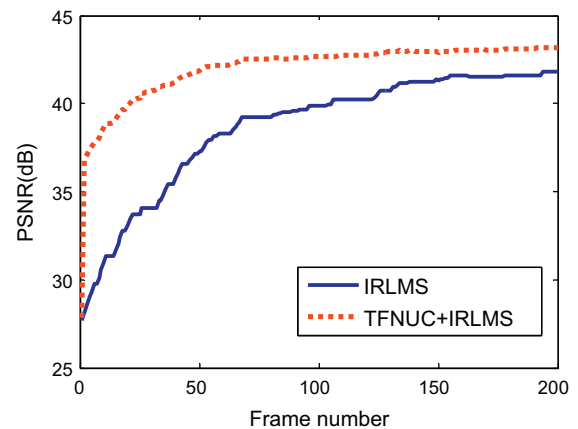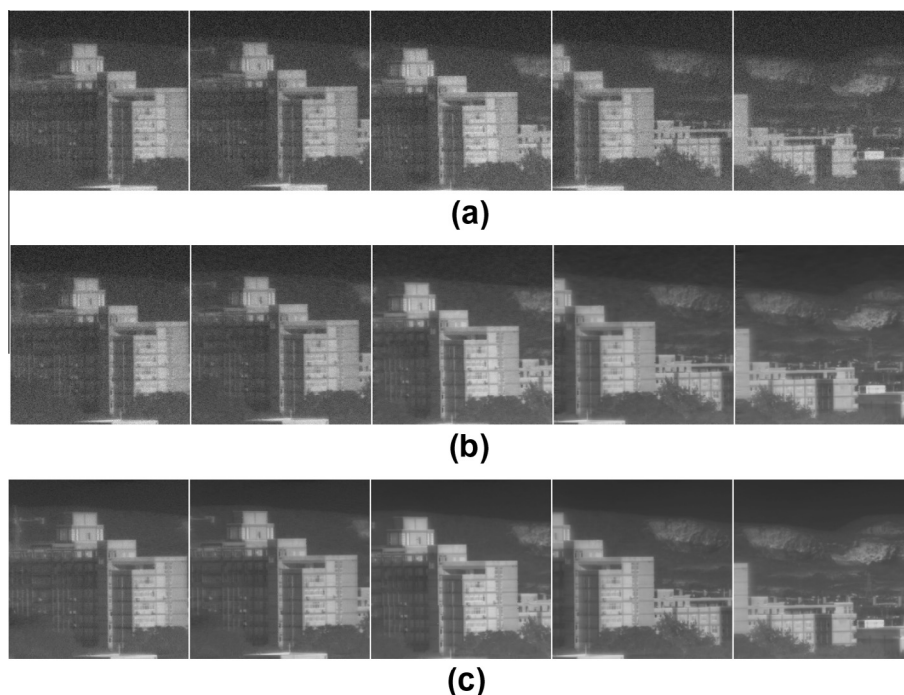

Fig. 8. PSNR comparison between the IRLMS and the combination method on the 200-frame synthetic noisy test sequence.

To validate the feasibility and validity of this idea, we conduct a simulation using another 200-frame clear video sequence, artificially

Fig. 9. The visual effect comparison of NUC results for 2nd, 10th, 40th, 100th, 200th frames (from left to right) from the video sequence. (a) Raw images. (b) IRLMS corrected images. (c) Combination method corrected images.

corrupted by the same level of Gaussian distributed FPN as in Section 3. Two methods are compared, first using IRLMS alone, and second method combining the proposed TFNUC with IRLMS – apply the TFNUC with the first two frames and then switch to IRLMS (using the offset estimated by TFNUC as the initial correction parameters) for recursively update the NUC parameter. The PSNR comparison is shown in Fig. 8. The raw frames 2, 10, 40, 100, 200 and their corresponding corrected versions are shown in Fig. 9. The correction video is also presented in Video 5. It can be seen by combining the two methods, the PSNR value directly jumped above 37 at first, and then gradually increased further, reaching 41.2 at frame 50. Then the algorithm began to converge after about 60th frame, and finally the value of PSNR reached 43.2 by the end of this sequence. While the using IRLMS alone, it took about 40 frames to pass the 35 dB barrier and at frame 200, there was still a 2 dB gap from the combination method. The PSNR results and the images displayed validate the feasibility and validity of using the proposed method as a first step fostering the success and accelerating the convergence process of more sophisticated registration-based time-evolving correction algorithms. It should be noted that although the time saved is not so much (only a few seconds); it may be very precious on some time-critical occasions.

Another problem existing in most time-evolving SBNUC methods is the NUC is performed based on sufficient global motion between the camera and the scene under observation. While for some special applications, e.g. fixed-spot IR surveillance, such kind of global motion is impractical. In this case, our method can be well applied because it only requires a very small relative scene motion and do not depend on larger scale global motion. Since the temporal drift of FPN is comparatively slow, the NUC can be performed periodically (e.g. every 1 min for one correction), by artificially introducing a small mechanical translation. Furthermore, compared with the "mechanical shutter" NUC approach, in which a uniform, and nontransparent surface covers the detector array periodically, our method is shutterless, and therefore free from the problems of image blocking or freezing.

Finally, since our method is based on registration, it also shares some limitations with most registration-based NUC methods. The validity of the proposed method is based on the following assumptions: (1) The infrared irradiance field of the observed scene remains unchanged during the two-frame time interval. (2) The scenes in the captured two frames exhibit only small global translations. These two assumptions should be met in order to guarantee a successful use of the TFNUC method.

5. Conclusions

In conclusion, we have presented a novel technique for scene-based nonuniformity compensation in FPA sensors. By using a pair of image frames with small relative translation, the NUC can be recast as a particular image restoration problem wherein the correction parameters are extracted by using the regularization-based constrained least-squares estimation. The unique advantages of the proposed method include that: it is direct, non-recursive, and employs only two image frames to obtain the NUC parameter without any assumptions on the structures of the FPN. Experiments on both simulated and real infrared data demonstrate the effectiveness of this technique. The future work will be focused on reducing its computational complexity for hardware implementation, and incorporating it within existing SBNUC methods to improve the real-time performance of practical imaging systems.

Appendix A. Supplementary material

Supplementary data associated with this article can be found, in the online version, at http://dx.doi.org/10.1016/j.infrared.2013.05.001.

References

[1] D.A. Scribner, K.A. Sarkay, J.T. Caulfield, M.R. Kruer, G. Katz, C.J Gridley, Nonuniformity correction for staring focal plane arrays using scene-based techniques, in: E. Dereniak, R.E. Sampson (Eds.), Infrared Detectors and Focal Plane Arrays, Proc. SPIE, 1990. vol. 1308, p. 224–233.

[2] D.A. Scribner, K.A. Sarkady, M.R. Kruer, J.T. Caulfield, J.D. Hunt, M. Colbert, M. Descour, Adaptive retina-like preprocessing for imaging detector arrays, in: Neural Networks, IEEE International Conference, vol. 1953; 1993, p. 1955–1960.

[3] D.A. Scribner, K.A. Sarkady, M.R. Kruer, J.T. Caulfield, J.D. Hunt, C. Herman, Adaptive nonuniformity correction for IR focal-plane arrays using, Neural Networks (1991) 100–109.

[4] J.G. Harris, C. Yu-Ming, Nonuniformity correction of infrared image sequences using the constant-statistics constraint, IEEE Trans. Image Process. 8 (1999) 1148–1151.

[5] S.N. Torres, M.M. Hayat, Kalman filtering for adaptive nonuniformity correction in infrared focal-plane arrays, J. Opt. Soc. Am. A 20 (2003) 470–480.

[6] S.N. Torres, R.A. Reeves, M.M. Hayat, Scene-based nonuniformity correction method using constant-range: performance and analysis, in: Proceedings of 6th World Multiconference on Systemics, Cybernetics and Informatics, vol. Ix, 2002, p. 224–229.

[7] R.C. Hardie, M.M. Hayat, E. Armstrong, B. Yasuda, Scene-based nonuniformity correction with video sequences and registration, Appl. Opt. 39 (2000) 1241–1250.

[8] B.M. Ratliff, M.M. Hayat, R.C. Hardie, An algebraic algorithm for nonuniformity correction in focal-plane arrays, J. Opt. Soc. Am. A 19 (2002) 1737–1747.

[9] C. Zuo, Q. Chen, G.H. Gu, X.B. Sui, Scene-based nonuniformity correction algorithm based on interframe registration, J. Opt. Soc. Am. A 28 (2011) 1164–1176.

[10] C. Zuo, Q. Chen, G.H. Gu, X.B. Sui, W.X. Qian, Scene-based nonuniformity correction method using multiscale constant statistics, Opt. Eng. 50 (2011).

[11] J.G. Harris, Y.M. Chiang, Minimizing the "ghosting" artifact in scene-based nonuniformity correction, Infrared Imaging Syst.: Des. Anal. Model. Test Ix 3377 (1998) 106–113.

[12] J.Q. Bai, Q.A. Chen, W.X. Qian, X.Y. Wang, Ghosting reduction in scene-based nonuniformity correction of infrared image sequences, Chin. Opt. Lett. 8 (2010) 1113–1116.

[13] W.X. Qian, Q. Chen, G.H. Gu, Space low-pass and temporal high-pass nonuniformity correction algorithm, Opt. Rev. 17 (2010) 24–29.

[14] C. Zuo, Q.A. Chen, G.H. Gu, W.X. Qian, New temporal high-pass filter nonuniformity correction based on bilateral filter, Opt. Rev. 18 (2011) 197–202.

[15] C. Zhang, W.Y. Zhao, Scene-based nonuniformity correction using local constant statistics, J. Opt. Soc. Am. A 25 (2008) 1444–1453.

[16] E. Vera, S. Torres, Fast adaptive nonuniformity correction for infrared focal-plane array detectors, Eurasip. J. Appl. Sig. P 2005 (2005) 1994–2004.

[17] A. Rossi, M. Diani, G. Corsini, Bilateral filter-based adaptive nonuniformity correction for infrared focal-plane array systems, Opt. Eng. 49 (2010).

[18] A. Rossi, M. Diani, G. Corsini, Temporal statistics de-ghosting for adaptive non-uniformity correction in infrared focal plane arrays, Electron. Lett. 46 (2010) 348–349.

[19] C. Zuo, Q. Chen, G. Gu, X. Sui, J. Ren, Improved interframe registration based nonuniformity correction for focal plane arrays, Infrared Phys. Techn. 55 (2012) 263–269.

[20] W.X. Qian, Q. Chen, G.H. Gu, Z.Q. Guan, Correction method for stripe nonuniformity, Appl. Opt. 49 (2010) 1764–1773.

[21] J. Ren, Q. Chen, W. Qian, G. Gu, C. Zuo, Efficient single image stripe nonuniformity correction method for infrared focal plane arrays, Opt. Rev. 19 (2012) 355–357.

[22] Y. Tendero, J. Gilles, S. Landeau, J.M. Morel, Efficient single image non-uniformity correction algorithm (2010) 78340E.

[23] M.R. Banham, A.K. Katsaggelos, Digital image restoration, Signal Process. Mag. IEEE 14 (1997) 24–41.

[24] R.C. Gonzalez, R.E. Woods, Digital Image Processing, third ed., Prentice-Hall Inc., 2006.

[25] C. Zuo, Q. Chen, G. Gu, X. Sui, Registration method for infrared images under conditions of fixed-pattern noise, Opt. Commun. 285 (2012) 2293–2302.

[26] B.R. Hunt, The application of constrained least squares estimation to image restoration by digital computer, IEEE Trans. Comput. 22 (1973) 805–812.